2022

Recursive Bayesian Calibration of Data-Driven Archetype Building Energy Models for Residential Sector: Application to a Research House

Seyed Matin Abtahi

Andreas K. Athienitis

Benoit Delcroix

Recursive Bayesian Calibration of Data-Driven Archetype Building Energy Models for Residential Sector: Application to a Research House

Seyed Matin ABTAHI[1]*, Andreas K. ATHIENITIS[1], Benoit DELCROIX[2]

[1]Centre for Zero Energy Building Studies, Department of Building, Civil, and Environmental Engineering, Concordia University,
Montréal, Québec, Canada
matinabtahi@gmail.com, andreask.athienitis@concordia.ca

[2] Hydro-Québec Research Centre, Laboratoire des Technologies de l'Energie (LTE), Shawinigan, Québec, Canada
delcroix.benoit@hydroquebec.com

* Corresponding Author

ABSTRACT

This paper studies recursive Bayesian calibration of archetype building energy models developed for optimal operation, energy flexibility and resilience in the residential sector. Real-time building performance monitoring has been facilitated recently with low cost faster instrumentations. With an online stream of measured data, recursive model calibration can be employed, where the model is initialized with prior knowledge and is updated with new measurements available to the building automation system. A Markov chain Monte Carlo approach is applied to calibrate two multi-zone archetype models with data from a research house in Québec. Most likely parameter values are estimated with an iterative Metropolis-Hastings algorithm over a 5-day train period and are validated by comparing the measured indoor air temperature in each zone with the model output over another 5-day test period. The time series of the posterior probability distribution shows that heat source activation influences the maximum likelihood values of most parameters and remarkably narrows down their associated credible intervals. Analyzing probability distribution time series helps understand the progression of acquired knowledge with new data and facilitates the comparison of various models.

1. INTRODUCTION

Archetype building/zone energy models are often used to evaluate the potential savings under near-optimal control strategies and system configurations; hence, recursive calibration is critical to ensure expected/promised savings. Calibration of archetype energy models based on sensor information is typically a non-convex offline (batch) optimization problem in which the parameters are estimated by minimizing the model error over a specific period. Alternatively, an online approach proposes initializing the model with prior knowledge and updating it with new measurements every time a sufficient number of data points are available to the building automation system (BAS). This approach enables monitoring the effect of outside ambient conditions and occupants' behaviour on uncertainty and identifiability of the parameters and establishes a direct link between new observations and information gained by the model.

Optimization techniques commonly assume the model parameters have fixed values and attempt to estimate them so that the model output fits the measurements as closely as possible. However, a Bayesian approach assumes the parameters have an underlying probability distribution and attempts to infer it by sampling from the solution space. Such an approach provides valuable insights regarding the inherent uncertainty in the model and its structural limitations. In this paper, we apply a Markov chain Monte Carlo approach – as a class of recursive Bayesian inference methods to update two multi-zone archetype energy models for (1) understanding the progression of information gain with new measurements and (2) detecting the structural shortcomings in the models.

2. METHODOLOGY

2.1 Case Study

The case study is an unoccupied research house – Experimental House for Building Energetics (EHBE) of Hydro-Québec, located in Shawinigan, Québec, Canada. This test bench is a two-storey detached house with an excavated basement. The house has outer dimensions of 7.6 m × 7.9 m and 60 m^2 footprint. It has three bedrooms and a bathroom on the second floor; the kitchen, the living room, the dining room and a small washroom are on the first floor. The wall assemblies of the building represent the typical lightweight wood-framed house in Québec. The total fenestration area is 20 m^2, consisting of vinyl framed double-glazing windows with an air gap. There are more than 150 sensors in the building and the soil around it. The available data consist of 15-minute average records of room-level electrical heating loads and 15-minute instant records of solar irradiance, outside ambient air temperature, soil temperature, and room-level indoor air temperature from 2019-01-01 to 2019-03-31.

2.2 Multi-Zone Archetype Energy Models

There are three main approaches to building energy modelling (Foucquier et al., 2013): 1) physics-based (white-box) approach, established on the principles of energy/mass conservation and heat transfer with comprehensive descriptions of building geometry, systems and material properties, 2) data-driven statistical (black-box) approach, based solely on mathematical models and measurements, with no assumption regarding the building physics and systems, and 3) hybrid (gray-box) approach, based on simplified building physics and systems performance, with parameters identified from measurements where simplified building geometry and information on the building energy systems reinforce the parameterization process. Gray-box models require much less data for calibration (Arendt et al., 2018) and are more likely to stay reliable outside the calibration range (Afroz et al., 2018) compared to black-box models. Compared to the white-box models, gray-box models are much faster to set up and calibrate. A gray-box model is not an oversimplification of the system topology but a selection of relevant information which requires 1) deep knowledge of the application and its physics and 2) coherent choice of significant states, inputs and disturbances (Abtahi et al., 2021). Essentially, an ideal gray-box model is the simplest one that describes all the dominant patterns and information embedded in the measurements (Bacher & Madsen, 2011). The computational simplicity and reasonable precision make gray-box models suitable for control applications.

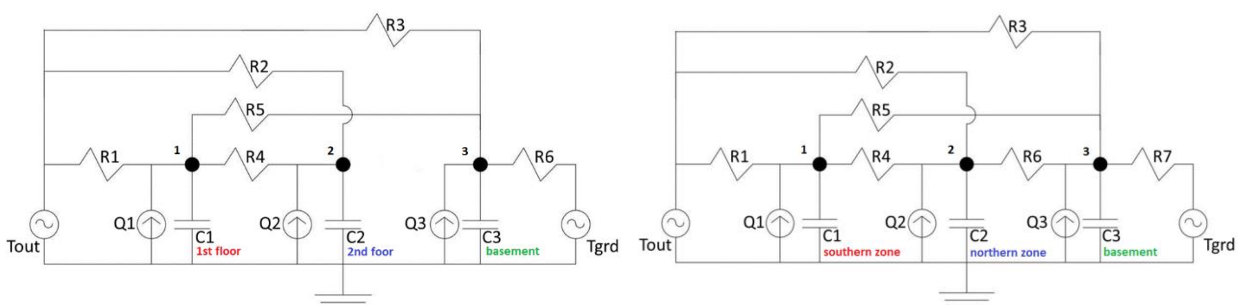

Figure 1. Left: 3C6R network model analogous to the zoning-by-floor approach – Right: 3C7R network model analogous to the zoning-by-orientation approach (Abtahi et al., 2021)

Authors have previously shown that a 3rd-order RC network model is sufficient to capture the fundamental thermal dynamics of typical single-family houses in Québec by developing two 3rd-order archetype models for the case study, with different approaches to discretize the building's indoor space (Abtahi et al., 2021): (1) Zoning-by-floor, i.e., to assume each floor of the building is a separate thermal zone. The assumption here is that the air inside each floor is thermally uniform, and the airflow between different floors is not significant; (2) Zoning-by-orientation, i.e., to assume the southern and northern zones of the above-grade space are separate thermal zones since the latter gains more solar radiation throughout the clear days, which effectively reduces its heating demand. Fig. 1-left shows the 3rd-order model analogous to the zoning-by-floor approach, where C_1, C_2 and C_3 represent the effective thermal capacity of the first floor, second floor and basement, respectively. Likewise, the model in Fig. 1-right shows the zoning-by-orientation approach where C_1, C_2 and C_3 represent the effective thermal capacity of the southern zone of the above-grade space, northern zone of the above-grade space and basement, respectively. T_{out} and T_{grd} are the outside ambient air temperature and average soil temperature, respectively.

These archetype models are adopted for this study, and the modelling steps are explained in the following. Eq. 1 is the differential equation governing the heat balance at any node (zone) *i* in the thermal RC networks, where C_i is the effective thermal capacity of zone *i*, Q_i is the aggregated heat flow to/from the air in zone *i*; *j* is all the zones connected to zone *i* by air, and R_{ij} is the thermal resistance between zone *i* and zone *j*. The weighted-average air temperature in any zone *i* is T_i. Eq. 2 is an explicit temporal discretization of Eq. 1, where *k* and *k*+1 indicate the current and the next time-step, respectively, and δt is the simulation time-interval.

$$C_i \frac{dT_i}{dt} = Q_i + \sum_j \frac{T_j - T_i}{R_{ij}} \tag{1}$$

$$T_i^{k+1} = \frac{\delta t}{C_i}\left(Q_i^{\,k} + \sum_j \frac{T_j^{\,k} - T_i^{\,k}}{R_{ij}}\right) + T_i^{\,k};\ \delta t \leq min\,\left(\frac{C_i}{\sum_j \frac{1}{R_{ij}}}\right) \tag{2}$$

2.3 Recursive Bayesian Calibration

Uncertainty is any deviation from the unachievable ideal based on deterministic knowledge about the system (Walker et al., 2003). Uncertainty sources are either aleatoric or epistemic (Iaccarino 2008). Aleatoric uncertainty is irreducible and refers to the inherently random nature of involved processes in the system. An example of an aleatoric source of uncertainty is the wind speed and direction patterns in a specific region. Epistemic uncertainty refers to the lack of knowledge in practice and can be reduced by conducting (additional accurate) measurements. For example, buildings' U-value is an epistemic source of uncertainty (Rastogi, 2016). In data-driven modelling, aleatoric and epistemic sources result in (1) experimental, (2) structural, and (3) identification uncertainty.

Experimental (observation) uncertainty is inevitable in the instrumentation and data acquisition process. Uncalibrated sensors, improper installment and communication failure in the acquisition system are among the more common sources of experimental uncertainty. Analyzing experimental uncertainty requires initializing the test/data collection many times under identical conditions.

Structural (model-inherent) uncertainty rises with insufficient knowledge of involved physical processes (e.g., unmeasured heating/cooling sources) and modelling simplifications. Common simplifications in gray-box models to facilitate the representation of buildings' thermal dynamics are linearization of heat transfer coefficients, spatial dimensionality reduction and temporal discretization (Athienitis & O'Brien, 2015). There is no generic methodology to deal with structural uncertainty due to its model-specific nature (Rajabally et al. 2002).

Identification (parameter) uncertainty refers to uncertainty in the model parameters given the available data. Analyzing identification uncertainty in building energy models is an active research topic with both frequentist and Bayesian approaches to probability and optimization. Bayesian inference methods suit control applications in buildings due to the capacity to monitor input signals' effect on parameter uncertainty in real-time. Table 1 summarizes the key differences between these two approaches:

Table 1: Key differences between frequentist and Bayesian approaches to probability and optimization (in the context of data-driven building energy modelling)

Frequentist Approach	Bayesian Approach
Suggests that probability can only be assigned to repeatable events, where the long-term frequency is measurable. Therefore, probability in the frequentist approach is related to the frequencies of repeated events.	Suggests that probability not only can be assigned to repeatable events but also helps express our belief about a particular subject given limited (sparse) observations. Therefore, probability in the Bayesian approach is related to our certainty/belief about the event/subject.
Assumes the model parameters have fixed values and attempts to estimate them so that the model output fits the observations as closely as possible.	Assumes the parameters have an underlying probability distribution and attempts to infer posterior distributions by sampling from the solution space. This approach does not perform a fit; instead, it explores the parameters space to determine their distributions without an explicit objective of refining the solution.

Calculates the variation of data (measurements) and the derived quantities given the fixed model. $P(data \mid model)$	Calculates the variation of certainty/beliefs about the model given the fixed data. $P(model \mid data) = P(data \mid model) \times \frac{P(model)}{P(data)}$
Makes a probabilistic statement about the intervals containing the unknown fixed parameter values; therefore, **Confidence** Intervals capture the uncertainty about the calculated intervals. *Example:* If the 95% Confidence Interval for the overall U-value of a house is 400 W/°C ± 10%, it means given the model, if the data is collected 100 times under near-identical conditions and the interval that contains the parameter value is computed, 95 of the 100 intervals fit in the range of 360 W/°C to 440 W/°C.	Makes a probabilistic statement about the model parameters within the desired solution region; therefore, **Credible** Intervals capture the current uncertainty in the parameter values. *Example:* If the 95% Credible Interval for the overall U-value of a house is 400 W/°C ± 10%, it means given the data, 95% of values that maximize the likelihood of observations and fit in the prior probability distribution are between 360 W/°C and 440 W/°C.

It is obvious from the example in Table 1 that the Bayesian approach is more intuitive for dealing with identification uncertainty in building energy modelling, as Credible Intervals address the uncertainty in parameter values and not the intervals containing them; also, collecting data under identical conditions is almost impossible. Bayesian inference methods are not adequate for fitting; however, they make it possible to thoroughly explore the parameter space around the solution after a fit has been done and help gain an improved understanding of the probability distribution. Bayesian methods refine the estimation of the most likely values for a set of parameters but do not iteratively find a better solution to minimize the model error.

For calibration, first, a uniform prior probability distribution of parameters (θ_i^0) is estimated from simplified geometry and material properties under certain assumptions about infiltration. Next, the prior probability distributions are updated by minimizing the model error over a training period with length N_{train}. Available data are transformed into the zone-level aggregated heat flow and weighted-average air temperature. HVAC output and solar gains are networked as aggregated heat flow ($\widehat{Q}_i$) to the zone air node as in Eq. 3, where $\widehat{Q}_{aux,i}$ is the measured heat delivered to the zone air, $\widehat{G}_{vert}$ is the measured global vertical irradiance on the southern façade, and α_i is the solar gain normalizer. Eq. 4 calculates the measured zone air temperature ($\widehat{T}_i$) by averaging the records of the sensors in the zone ($\widehat{T}_{s,i}$) weighted by the floor area covered by each sensor (A_s), where *s* is all the sensors in zone *i*. The result of the least-square minimization in Eq. 5 is the input prior probability distribution to the Metropolis-Hastings algorithm ($N_i = 3$).

$$\hat{Q}_i = \hat{Q}_{aux,i} + \alpha_i \hat{G}_{vert} \tag{3}$$

$$\hat{T}_i = \sum_s A_s \hat{T}_{s,i} / \sum_s A_s \tag{4}$$

$$\begin{gathered} \min_{\theta_i} \sum_{i=1}^{N_i} \sqrt{\sum_{k=1}^{N_{train}} \left(T_i{}^k - \hat{T}_i{}^k\right)^2 / N_{train}} \; ; \theta_i = \left[R_{i,j}, C_i, \alpha_i\right] \\ \textit{subject to:} \\ \underline{\theta_i} < \theta_i < \overline{\theta_i} \\ T_i{}^{k+1} = T_i{}^k + \left(\frac{\delta t}{C_i}\right)\left(\hat{Q}_i{}^k + \sum_j \frac{T_j - T_i}{R_{ij}}\right) \; k \in N_0{}^{N_{train}-1} \end{gathered} \tag{5}$$

The Metropolis-Hastings algorithm takes random samples from the parameter space regarding this prior probability distribution and refines the prior knowledge about the model by calculating a Credible Interval for the values that maximize the likelihood of given data. First, an ensemble of Markov chains is formed starting from relatively distant arbitrary points. Each chain is a stochastic process of one walker that moves around randomly in the parameter space using a proposal distribution for new steps and a policy for rejecting a fraction of the proposed moves. Therefore, the proposal distribution for each walker's new steps depends on the other walkers' relative situation. The ensemble evolves through the parameter space and shapes a posterior probability distribution. The more steps are included in the ensemble evolution, the more closely the posterior distribution matches the actual (real-life) distribution. However, as the ensemble's first steps (burn-in phase) may not reflect the posterior distribution, they must be discarded.

The choice of the proposal distribution and a proper initialization are critical for the algorithm's performance. Determining the number of steps required to converge to the stationary distribution within an acceptable uncertainty is a challenging task. Given an improper rejection policy, the ensemble convergence can take a long time as the walkers may double back and explore the space already covered.

3. EVALUATION OF METHODOLOGY

Electric space heating is widely adopted in the Québec residential sector and strongly influences the region's demand profile during cold winters. The grid's peak demand periods typically occur on extremely-cold weekday mornings from 6:00 to 9:00 (when people wake up, get ready and leave home) and evenings from 16:00 to 20:00 (when people return home, cook and rest), during which space heating stresses the grid the most. A newly introduced dynamic tariff (rate flex-D) gives the residential customers in Québec the opportunity to actively reduce the pressure on the grid and save money during the peak periods by shifting the load to the off-peak periods when electricity is approximately 12 times cheaper. Archetype energy models help residential customers take cost-optimal actions; hence, recursive calibration is critical to ensure expected savings.

The training data needs to comprise enough information regarding the building thermal dynamics within the comfort range. Therefore, a 5-day period (N_{train} = 120h) from March 2019 is selected, during which the indoor air temperature in each zone varies due to variable levels of auxiliary heat and solar gains. There is also a period of free-floating indoor air temperature, which helps understand the effect of heat source activation on the maximum likelihood values and credible intervals. The trained model is then tested over another 5 days (N_{test} = 120h) of the same month to validate its ability to predict the indoor air temperature in each zone. Figure 1 presents the training data.

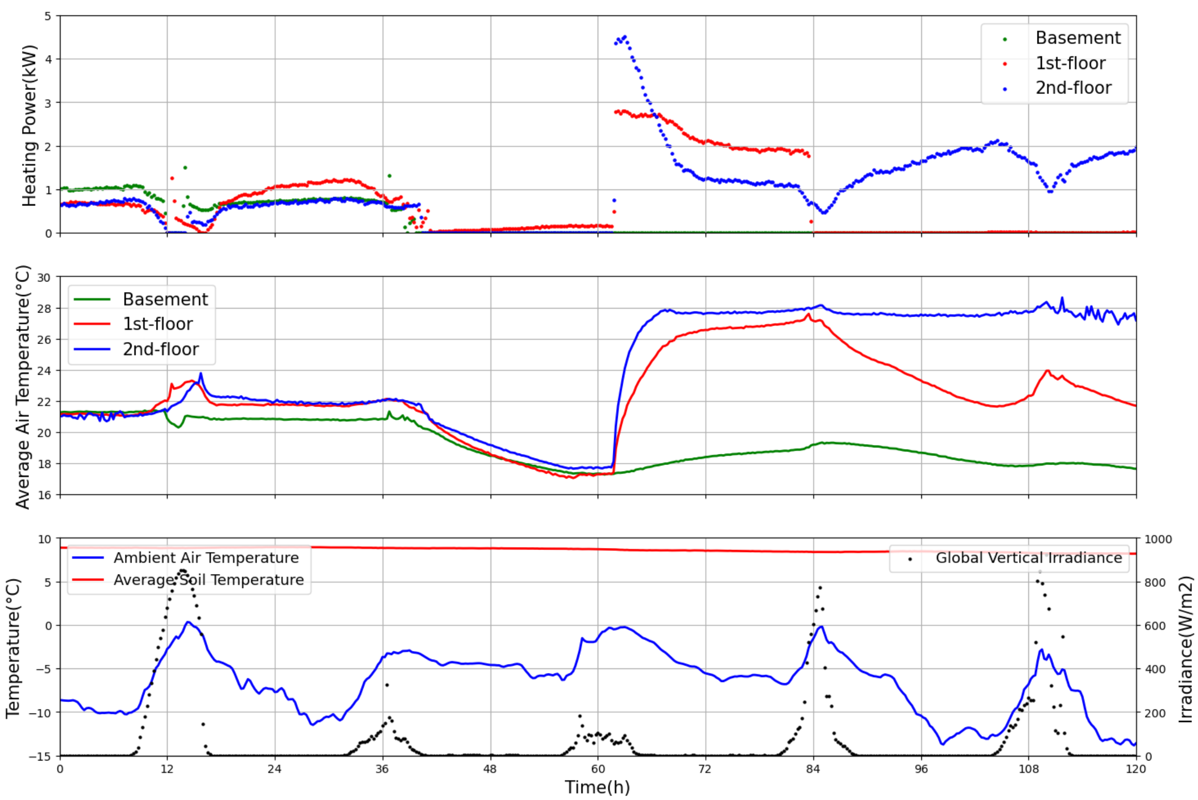

Figure 2. Training data

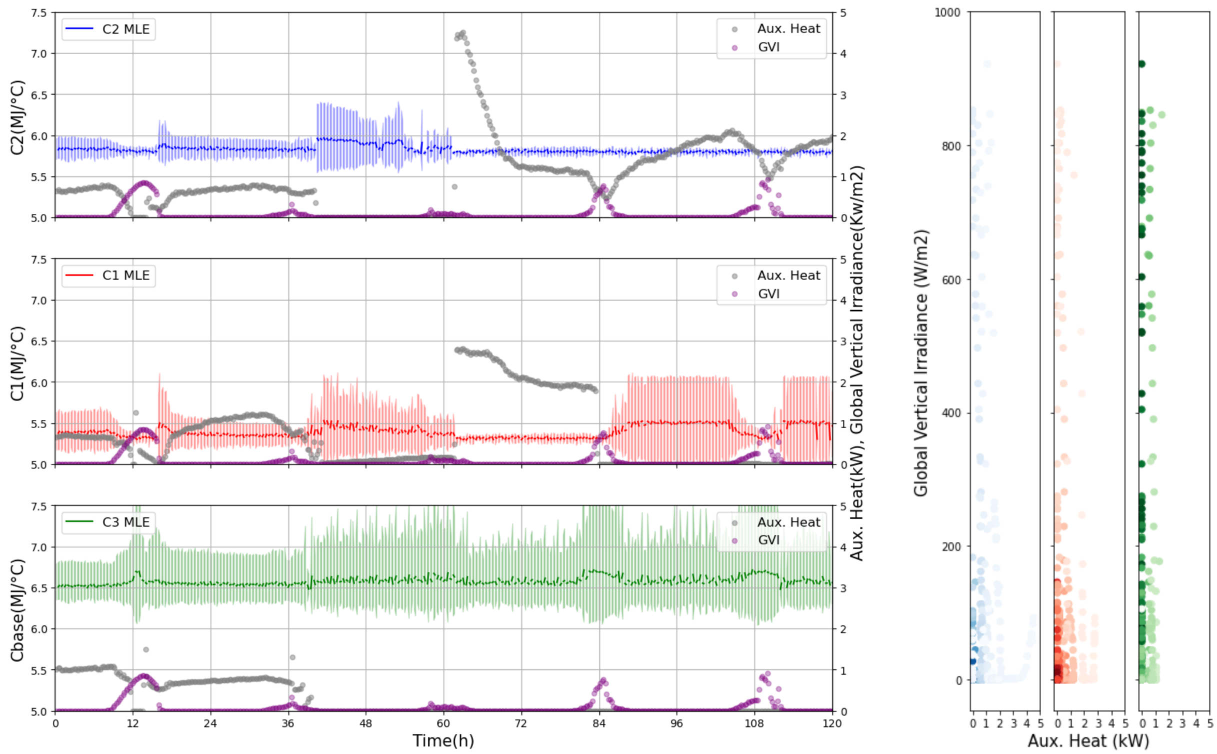

Figure 3. Time series of 95% Credible Interval and Maximum Likelihood Estimation (MLE) for effective thermal capacity of different zones: 3C6R model (left) – Corresponding normalized uncertainty (right)

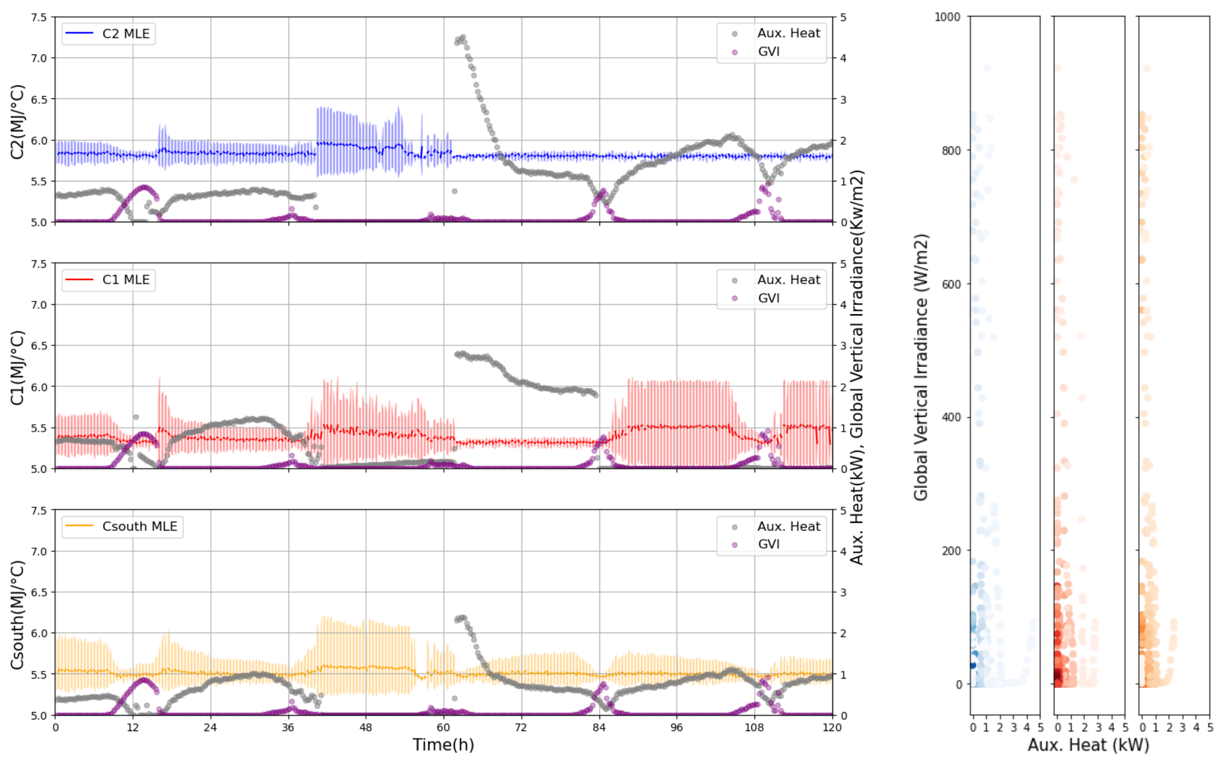

Figure 4. Time series of 95% Credible Interval and Maximum Likelihood Estimation (MLE) for effective thermal capacity of different zones: 3C6R model vs. 3C7R model (left) – Corresponding normalized uncertainty (right)

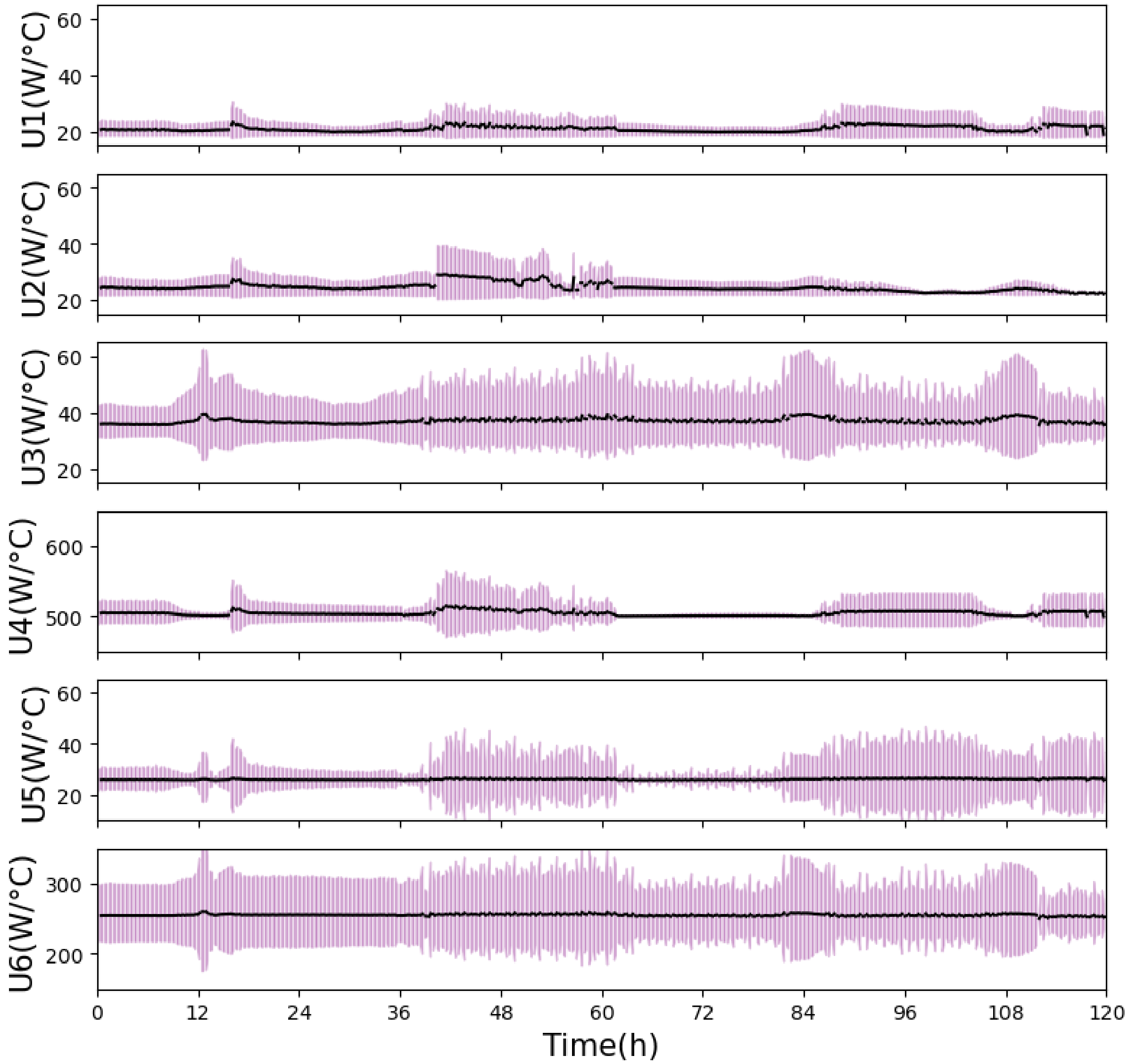

Figure 5. Time series of 95% Credible Interval and Maximum Likelihood Estimation (MLE) for thermal conductance between zones and surroundings: 3C6R model

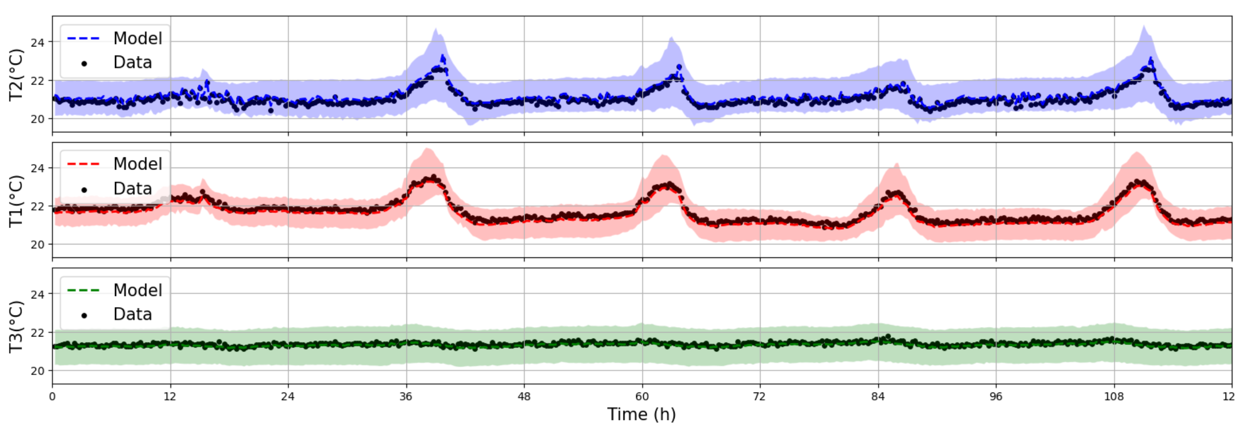

Figure 6. Predicted vs. measured indoor air temperature: 3C6R model (from top to bottom: second floor, first floor, basement. The highlighted band shows the uncertainty due to propagation of the probability distributions)

Figure 3-left presents the posterior probability distribution time series for the effective thermal capacity of the basement, first floor and second floor. Progression of 95% Credible Intervals shows an inverse correlation between activation of heat sources and parameters uncertainty. As the auxiliary heat turns off, the only intermittent heat source is the solar gains which are negligible unless it is a clear day. Therefore, the energy flow through RC networks in free-float conditions is much less than what it is in the presence of auxiliary heat. This provides less information to capture per unit of time and as a result, credible intervals start wide-ranging, which interprets to less certainty in the parameter values and models' output. Figure 3-right colour maps the normalized uncertainty of C_1, C_2 and C_3 (3C6R model) with regard to heat sources, where darker points represent less certain (more uncertain) values and vice-versa. This figure emphasizes the mentioned inverse correlation.

Figure 4 shares the concept with figure 3, however, it compares the thermal capacity of the air in the first and second floors from the 3C6R model (C_1 and C_2) with the thermal capacity of the air in the southern zone from the 3C7R model (C_{south}). Figure 4-right implies that the uncertainty of C_{south} is more dependent on the global vertical irradiance on the southern façade compared to C_1 and C_2, which verifies the idea of two different approaches to discretize the building's indoor space.

Figure 5 presents the time series of 95% Credible Interval and Maximum Likelihood Estimation (MLE) for thermal conductance between zones and surroundings (3C6R model), where $U_{ij} = 1/ R_{ij}$. This figure shows the probability distribution of U_{grd} ($1/R_{grd}$) does not change much, which means that given the training data, this parameter is non-identifiable. Generally, analyzing posterior distribution time series helps understand how models capture information with new data, what factors critically influence the uncertainty and what structural shortcomings exist in the model.

Finally, to validate the accuracy and interpretability of the methodology, the measured indoor air temperature in each floor is compared to the corresponding output of the 3C6R model over a 5-day test period. Figure 6 shows the model's outputs given the MLE and its uncertainty due to propagation of the posterior probability distribution.

4. CONCLUSIONS

This paper presented a methodology for recursive Bayesian calibration of simple archetype house energy models in the Québec residential sector. Two 3rd-order RC network models were adopted to capture the thermal dynamics of the case study, which is an unoccupied two-story research house. One model (3C6R network) assumes that each floor is a separate thermal zone, and the other model (3C7R network) assumes that the south-facing zone and the north-facing zone of the above-grade space are separate thermal zones. A Markov chain Monte Carlo approach is applied to recursively calibrate these archetype models over a 5-day train period. Minimizing the models' error in the prediction of the indoor air temperature over the training period provides a prior probability distribution, which is later refined by random sampling from the parameter space with an iterative Metropolis-Hastings algorithm.

Progression of the posterior probability distributions in time shows that activation of auxiliary heat and solar gains influences the maximum likelihood values of most parameters and effectively reduces their associated uncertainty. The training data comprised a period of free-floating indoor air temperature to investigate the effect of heat source deactivation on the credible intervals. As the auxiliary heat turns off, the only intermittent heat source is the solar gains which are negligible unless it is a clear day. Therefore, the energy flow through RC networks in free-float conditions is much less than what it is in the presence of auxiliary heat. This provides less information to capture per unit of time and as a result, credible intervals start wide-ranging, which interprets to less certainty in the parameter values and models' output.

Comparing the two models shows that zoning the above-grade space by orientation and dividing it into the southern and northern zones increases the dependence of thermal capacitances uncertainty on the global vertical irradiance on the southern façade, meaning that the 3C7R model uncertainty is more sensitive to the vertical irradiance patterns than the 3C6R model uncertainty. Generally, analyzing posterior distribution time series helps understand how models capture information with new data, what factors critically influence the uncertainty and what structural shortcomings exist in the model. In the end, to validate the accuracy of the methodology, the measured indoor air temperature in each zone is compared to the corresponding model output over a different 5-day test period.

NOMENCLATURE

$\hat{G}_{vert}$	Measured global vertical irradiance on the southern façade (W/m^2)
$\hat{Q}_{aux,i}$	Measured heat delivered to the air in zone *i* (W)
$\hat{Q}_i$	Measured aggregated heat flow to the air in zone *i* (W)
$\hat{T}_i$	Measured weighted average air temperature of zone *i* (°C)
$\hat{T}_{s,i}$	Measured air temperature by sensor *s* in zone *i* (°C)
A_s	Floor area covered by sensor *s* (m^2)
C_i	Thermal capacity of the air in zone *i* (J/°C)
N_i	Number of the zones in the RC network (-)
N_{test}	Testing period length (sec)
N_{train}	Training period length (sec)
R_{ij}	Thermal resistance between zone *i* and zone *j* (°C/W)
T_{grd}	Average soil temperature (°C)
T_i	Predicted weighted average air temperature of zone *i* (°C)
T_{out}	Outside ambient air temperature (°C)
α_i	Solar gain normalizer of zone *i* (-)
δt	Simulation time-interval (sec)
θ_i	RC network parameters related to zone *i* (-)

REFERENCES

Abtahi M, Athienitis A, Delcroix. Control-oriented thermal network models for predictive load management in Canadian houses with on-Site solar electricity generation: application to a research house. Journal of Building Performance Simulation 2021. doi:10.1080/19401493.2021.1998223.

Afroz Z, Shafiullah G. M, Urmee T, Higgins G. Modeling techniques used in building HVAC control systems: A review. Renewable and Sustainable Energy Reviews 2018; 83:64–84.

Arendt K, Jradi M, Shaker H. R, Veje C. Comparative analysis of white, gray and black-box models for thermal simulation of indoor environment: Teaching building case study. Proceedings of the 2018 building performance modelling conference and simbuild co-organized by ASHRAE and IBPSA-USA; 173–180.

Athienitis A. K, O’Brien W. (2015). *Modelling, Design, and Optimization of Net-Zero Energy Buildings*. Wiley.

Bacher P, Madsen H. Identifying suitable models for the heat dynamics of buildings. Energy and Buildings 2011; 43:1511–22.

Foucquier A, Robert S, Suard F, Stephan L, Jay A. State of the art in building modelling and energy performance prediction: A review. Renewable and Sustainable Energy Reviews 2013; 23:272–88.

Iaccarino G. Quantification of Uncertainty in Flow Simulations Using Probabilistic Methods. VKI Lecture Series - Sept. 8-12, 2008.

Rajabally, E., P. Sen, and S. Whittle (2002). “A methodology for model dependability assessment.” In: Proceedings of the Computer-Based Design: Engineering Design Conference 2002, pp. 291–300.

Rastogi P. On the sensitivity of buildings to climate: the interaction of weather and building envelopes in determining future building energy consumption. PhD thesis. EPFL, Lausanne, Switzerland 2016.

Walker, W. E., P. Harremoes, J. Rotmans, J. P.v. d. Sluijs, M. B.A. v. Asselt, P. Janssen, and M. P.K. v. Krauss (2003). "Defining Uncertainty: A Conceptual Basis for Uncertainty Management in Model-Based Decision Support." In: Integrated Assessment 4, pp. 5–17. doi:10.1076/iaij.4.1.5.16466.

ACKNOWLEDGEMENT

The financial support through an NSERC/Hydro-Québec Industrial Research Chair is gratefully acknowledged. The authors would also like to thank the research team at Hydro-Québec Research Centre Laboratoire des Technologies de l'Energie for providing the data and valuable suggestions.